GEOCHRONOMETRIA 41(3) 2014: 278–293
DOI 10.2478/s13386-013-0154-1

Available online at
www.springerlink.com

ABSOLUTE CHRONOLOGY OF FLUVIAL EVENTS IN THE UPPER DNIEPER RIVER SYSTEM AND ITS PALAEOGEOGRAPHIC IMPLICATIONS

ANDREY V. PANIN[1], GRZEGORZ ADAMIEC[2], KHIKMATULLA A. ARSLANOV[3], MARIA A.BRONNIKOVA[4], VLADIMIR V. FILIPPOV[1], ELENA D. SHEREMETSKAYA[1], NATALYA E. ZARETSKAYA[5] and ELYA P. ZAZOVSKAYA[4]

[1]*Faculty of Geography, Moscow State University, Vorobiovy Gory 1, Moscow, 119991, Russia*
[2]*GADAM Centre of Excellence, Silesian University of Technology, Krzywoustego 2, 44-100, Gliwice, Poland*
[3]*Faculty of Geography and Geoecology, Sankt-Petersburg State University, 10th Line, house 33, Sankt-Petersburg, 199178, Russia*
[4]*Institute of Geography, Russian Academy of Sciences, Staromonetny Per. 29, Moscow, 119017, Russia*
[5]*Geological Institute, Russian Academy of Sciences, Pyzhevsky Per. 7, Moscow, 119017, Russia*

Received 8 August 2013 Accepted 25 November 2013

Abstract: A set of 121 radiocarbon and OSL dates has been compiled from the Upper Dnieper River and tributary valleys, Western European Russia. Each date was attributed according to geomorphic/sedimentological events and classes of fluvial activity. Summed probability density functions for each class were used to establish phases of increasing and reducing fluvial activity. The oldest detected reduction of fluvial activity was probably due to glacial damming at LGM. Within the Holocene three palaeohydrological epochs of millennial-scale were found: (1) high activity at 12,000–8,000 cal BP marked by large river palaeochannels; (2) low activity at 8,000–3,000 cal BP marked by formation of zonal-type soils on -floodplains; short episodes of high floods occurred between 6,500–4,400 cal BP; (3) contrasting hydrological oscillations since 3,000 cal BP with periods of high floods between 3,000–2,300 (2,000) and 900–100 cal BP separated by long interval of low floods 2,300 (2,000)–900 cal BP when floodplains were not inundated — zonal-type soils were developing and permanent settlements existed on floodplains. In the last millennium, four centennial-scale intervals were found: high flooding intervals are mid-11–mid-15th century and mid-17–mid-~~20th~~ 19th century. Intervals of flood activity similar to the present-day were: mid-15–mid-17th century and since mid-19th century till present. In the context of palaeohydrological changes, discussed are selected palaeogeographic issues such as: position of the glacial boundary at LGM, role of changing amounts of river runoff in the Black Sea level changes, floodplain occupation by Early Medieval population.

Keywords: glacial damming, Holocene palaeohydrology, palaeofloods, buried floodplain soils, Dnieper River, Black Sea.

Corresponding author: A. V. Panin
e-mail: a.v.panin@yandex.ru

ISSN 1897-1695 (online), 1733-8387 (print)

1. INTRODUCTION

In the last two decades, large arrays of absolute age determinations have been widely used to extract geomorphic and hydrologic signals from the past. Frequency distribution of radiocarbon dates from river floodplains provided uncovering periods of active sedimentation (alluviation) and high flooding in Britain (Macklin and Lewin, 1993, 2003), Spain (Thorndycraft and Benito, 2006), Poland (Starkel *et al.*, 2006) and Germany (Hoffmann *et al.*, 2008). Revelation of river regime variations in the Holocene based on statistical treatment of radiocarbon dates has become a tool for correlation of palaeohydrological phenomena at sub-continental scale (Macklin *et al.*, 2006) and studying hydrological responses to climate and land use changes (Macklin *et al.*, 2005; Johnstone *et al.*, 2006; Starkel *et al.*, 2006; Hoffmann *et al.*, 2008).

Since the late 1990s, a big collection of absolute age determinations has been accumulated from the Upper Dnieper river and its tributaries within the Smolensk Region (Russia). Dnieper is the third largest river in Europe with today's length of 2200 km (2290 km before construction of reservoirs) and catchment area of 512 000 km^2, which discharges into the Black Sea on average 53 km^3 of water annually (Sukhodolov *et al.*, 2009). Dnieper starts in the Valdai Hills in North-Western Russia along with Rivers Volga and Western Dvina (Daugava) that flow to the Caspian Sea and Baltic Sea respectively (**Fig. 1**). Due to its geographic position at the triple divide, the Upper Dnieper fluvial system has being involved into palaeoenvironmental context far outside the catchment boundaries (**Fig. 1**).

Fluvial history of the Dnieper River and its tributaries has been studied in Byelorussia (Kalicki and Sańko, 1992, 1998; Kalicki 1995, 2006; Kalicki *et al.*, 2008), in the Dnieper's left tributary catchments (Panin *et al.*, 2001; Borisova *et al.*, 2006). Nevertheless, a systematic chronology of fluvial events in the Dnieper River system has not been proposed yet. Not the last reason why it has not been done is the lack of absolute chronology data that had existed till now. In the last decade, a large number of radiocarbon and OSL dates have been obtained by the authors. This data set when statistically treated is potentially perspective to obtain information on fluvial history which value extends beyond the Dnieper river system itself. In this paper we aim at geomorphic and palaeohydrologic evaluation of these dates, establishing chronology of fluvial events and linking it to regional palaeogeographic context, namely the LGM and postglacial delivery of freshwater to the Black and Caspian Seas and river regime in the Holocene.

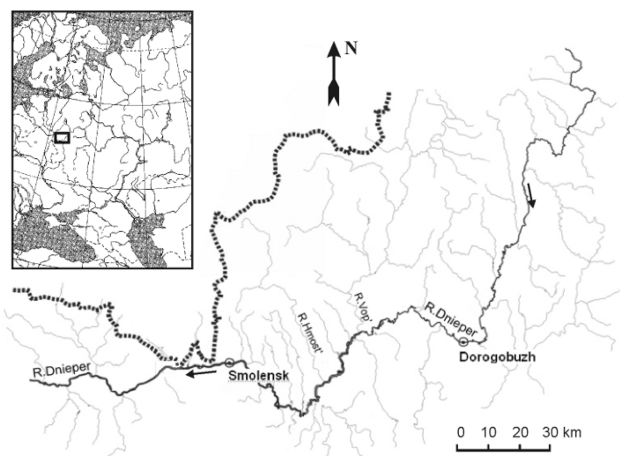

Fig. 1. *Dashed line — ice sheet margin during LGM (after Barashkova* et al.*, 1998).*

2. STUDY SITE

At Smolensk the Upper Dnieper River has catchment area of 14 100 km^2, mean annual discharge 97 m^3/s, mean maximum discharge 1990 m^3/s. Seasonal amplitude of river level reaches 10 m with highest levels occurring during the spring snowmelt flood and low water seasons in summer and winter. River channel makes irregular meanders divided by long relatively straight segments (**Fig. 2**).

The Dnieper River valley at its upper course was formed in the end of OIS-6 after the territory was left by the Moscovian (Late Saalian) ice sheet. In the Early Valdai (Early Vistulian, OIS-4) epoch the ice margin was far from the valley, but during the Late Valdai (Late Vistulian, OIS-2) time valley was subject to direct influence of the ice sheet. During the Last Glacial Maximum (LGM, 23–20 ka cal BP) the ice margin was located in the vicinity of the upper Dnieper valley (**Fig. 1**). Upstream from Smolensk it stayed 50–70 km to north/north-west from the valley. Glacial melt waters were transported to the Dnieper valley via its right tributaries — rivers Vop', Hmost', *etc.* and contributed much both to water and to sediment discharge of the Dnieper River. Downstream from Smolensk the LGM ice margin approached the Dnieper valley and according to some authors (Salov, 1972; Kvasov, 1979) could have crossed the valley which resulted in formation of a glacial dammed lake. Well pronounced esker/kame ridge lying across the right-side low river terrace at the Katyn' town 15 km downstream from Smolensk (**Fig. 2**) supports this view.

Clear alluvial surfaces at the valley reach around Smolensk are presented by the low terrace (10–14 m above the river) and floodplain (5–9 m). Morphology of the low terrace provides its subdivision into two generations of different ages that do not clearly differ in elevation but can be designated in surface morphology and cover sediments (**Fig. 2**). The older part of the terrace has low relief and unclear fluvial topography and is covered by a thin (typically <1 m) shawl of loess-like silts. There are not absolute dates from channel alluvium of this terrace, but its blocking by glacio-fluvial ridge at Katyn'

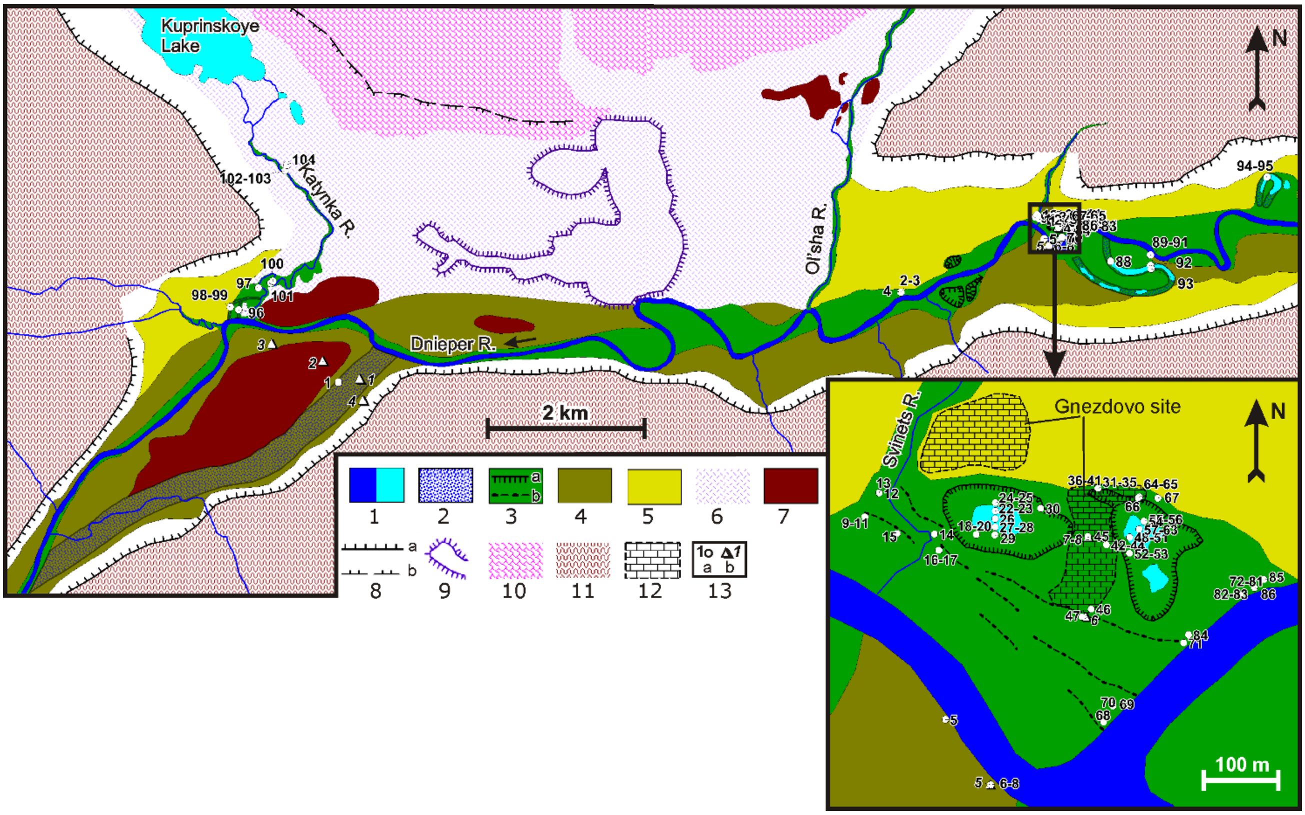

Fig. 2. *Geomorphic map of a selected section of the Upper Dnieper valley with location of dated cores and exposures. Numbers correspond to date numbers in Tables 1 and 2.*

Legend: 1 — modern hydrographic objects: Dnieper river channel, lakes, small rivers; 2 — palaeochannels; 3 — floodplain terrace (5-9 m) with individual topographic elements (a — erosion pits, b — levees); 4 — 10–13 m loess-devoid terrace (Late Glacial — Early Holocene); 5 — 10–14 m loess-covered terrace (LGM); 6 — alluvial valley bottoms reworked by glacio-fluvial processes (LGM); 7 — erosion remnants composed of glacial tills of different ages; 8 — valley shoulders and valley sides (a — contemporary, b — pre-LGM, visible through glacial/glacio-fluvial sedimentary cover); 9 — glacio-fluvial ridges (eskers), LGM; 10 — morain terrain of the Late Valdaian glaciation (MIS 2); 11 — partly reworked morain/glacio-gluvial terrain of the Moscovian glaciation (MIS 6); 12 — living space of the Gnezdovo Early Medieval settlement; 13 — location of dated samples (a — ^{14}C, b — OSL) and their numbers in Tables 1, 2.

Note: elevation of river terrace are related to the Dnieper valley and expressed in meters above the river at typical low-water stage.

confirms its LGM age The younger part of the low terrace at Smolensk bears clear levee-hollow topography with up to 3 m relief. It was dated to the Late Glacial — Early Holocene time (this study). The 10 m Dnieper terrace some 100 km downstream Smolensk at the Orsha city (Byelorussia) has also post-LGM age as follows from the radiocarbon date of 17150 ± 300 BP (uncal) that was obtained from lacustrine silts underlying terrace alluvium (Kalicki and Sańko, 1992).

Floodplain at the Smolensk section of the valley contains only few palaeochannels (**Fig. 2**), but bears also large erosion pits that evidence powerful palaeofloods (**Fig. 2**, inset). These features are characteristic for the older (Mid-Holocene) part of the floodplain, which outside these forms exhibits low-relief surface smoothed by overbank sedimentation. The Late Holocene floodplain is featured by levee-hollow topography produced by active lateral migration of the channel. Both generations of the floodplain constitute the major archives of the river Holocene palaeohydroogy both in their sedimentology (buried soils and overbank alluvium) and geomorphic features which parameters allow their interpretation in palaeohydrological terms.

3. METHODS

The study has been conducted in three stages.

Stage 1. Collection of the data base. The gathered set of dates refers to the Russian part of the Upper Dnieper and tributary valleys. A big part of them was obtained at a short valley segment downstream from Smolensk during the multi-disciplinary research of the Gnezdovo archaeological site, an Early Medieval Scandinavian settlement in the Dnieper valley, one of key stops at the trade route “from Varangians to the Greeks” that was linking Scandinavia and the Byzantine Empire. All dates have been verified by independent data — sedimentary and geomorphic settings, pollen analysis of sediments.

The dates that do not correspond to local stratigraphy, including inverse dates, were excluded from further analysis. In total, there remained 121 entries: 110 radiocarbon (**Table 1**) and 11 OSL dates (**Table 2**). Few of them have already been published elsewhere but most of the dates have so far been presented in technical reports and conference abstracts only. The majority of the dates are published here in a paper form for the first time.

To avoid bias generated by land use and disturbance of natural sedimentary contexts, dates directly correlated with archaeological sites have been excluded from analysis in some studies (Macklin and Lewin, 2003; Hoffman *et al.*, 2008). In the Upper Dnieper catchment cultural layers from Early Medieval settlements located on river floodplains can be clearly associated with sedimentation history as their economical and living patterns revealed by archaeologists (Pushkina *et al.*, 2001; Murasheva *et al.*, 2009) evidence that they existed in the absence of flooding. We therefore do use the dates from cultural layers of permanent settlements to specify temporal limits of low flooding intervals.

Stage 2. Division of dates into classes according to fluvial activity. There have been several approaches proposed to classify absolute dates in terms of fluvial dynamics and/or palaeoflood hydrology.

1) The "active" – "passive" dates approach with the former ones presenting any sediment that is accumulated in fluvial environment, and the latter exhibiting time spans with no minerogenic sedimentation occurring (ex., dates on peats or buried soils). This approach was used to find the chronology of erosion events on slopes, gullies and dry valleys, *i.e.* in simply organized one-dimensional erosion/sedimentation systems (Lang, 2003; Panin *et al.*, 2009). In riverine environments this approach is applicable if sedimentation is known for its discontinued temporal pattern. This is true for bedrock channels where any date from slackwater deposits indicates an extreme flood event (Harden *et al.*, 2010). Alluvial channels require a more sophisticated procedure.
2) The "change" dates approach. It consists in separating dates into different depositional environments (channel deposits, abandoned channels, overbank sedimentation, flood basins) and extracting ones that relate to geomorphologically significant changes in river activity within each group (Macklin and Lewin, 2003). Such dates called "change dates" (Macklin *et al.*, 2006) refer, for example, to overbank sediments that bury floodplain soils or floodplain mire peats. Thorndycraft and Benito (2006) complement the above list of depositional environments with slackwater flood deposits. This approach allows identifying major flood episodes and periods of low flood activity as troughs in flood record.
3) The facial interpretation of dated sediments in terms of fluvial activity/stability (Hoffmann *et al.*, 2008). The advantage of this approach is that a large data set on geomorphic results of river flooding can be used such as dates on channel avulsions. Further development of this approach consists in accounting for sedimentary context with separate processing of dates from within the alluvial units (change dates — the ones taken from the base of alluvial unit, the midpoint dates — those taken from middle of alluvial sequence) and the dates that bracket sedimentation events — "bracketing dates" (Thorndycraft and Benito, 2006). The 8-member classification of depositional environments in Starkel *et al.* (2006) combines the sedimentary environment and sedimentary context (relation of date to flood event). Observations on recent floodplain accretion reveal strong dependence of sedimentation rates on site position relative to the river (Golosov, 2009; Belyaev *et al.*, 2013; *etc.*). Therefore, in order to be able to interpret changes in floodplain accretion rate in terms of flooding history, lateral migration of river channel should be taken into account.

To use advantages of each of the above approaches we tried to put each date into the context of specific hydrologic event or state of river channel in comparison to the present. This task was achievable due to the authors having collected almost all of the dated samples themselves and being aware of the details of section/ core location. We grouped all the dates into three classes of fluvial activity with the present-day river regime, sedimentation style and channel parameters taken as the reference. Each activity class was designated from the following geomorphic and sedimentation indications, some of them being rather widespread (such as buried soils), the others being specific for the studied valley reaches:

1) Low activity (LA) indicated by:
   a) overbank sedimentation is weak or not occurring at all (floodplain peats, well developed soils);
   b) small size of river palaeochannels;
   c) lacustrine environments over the valley bottom (oxbows are not included).
2) Medium activity (MA), *i.e.* geomorphic and sedimentation events which magnitude is similar to that of the present-day river:
   a) active overbank sedimentation at low floodplain levels, in floodplain hollows and in palaeochannels with limited sedimentation at high floodplain levels;
   b) channel size and pattern similar to the present-day channel;
   c) lateral river migrations of modern rate and type.
3) High activity (HA):
   a) unusually active overbank sedimentation;
   b) erosion over valley bottoms produced by extremely powerful floods;
   c) large palaeochannels.

Table 1. *Radiocarbon dates from the upper Dnieper River and tributary valleys.*

			Calibrated age		Core/section location						Sample characteristics			Fluvial events[4]			Fluvial activity class[5]			
No.	Index	14C age (BP)	68.2% interval (BC/AD)	M±s (cal BP)	Name	Latitude (°N)	Longitude (°E)	Absolute height (m)	Elevation above the river (m)	Geomorphology[1]	Depth (m)	Stratigraphy[2]	Dated material[3]	post-dated	dated	pre-dated	post-dated	dated	pre-dated	Source[6]
River Dnieper																				
1	GIN-14375	7450 ± 320	6660BC–5980BC	8330 ± 350	Gn-10-21	54.75739	31.72718	169.5	9.5	TP	2.10–2.20	OB+BP, foot	P	33			H			1
2	IGAN-2546	90 ± 30	1690AD–1920AD	130 ± 80	P-20-00	54.76897	31.84044	166.5	6.0	F	0.04	OB+BS	H/B		21			M		4
3	IGAN-2545	940 ± 90	1010AD–1190AD	850 ± 90	P-20-00	54.76897	31.84044	166.5	6.0	F	0.72–0.93	BS+CL	H/B		11			L		1
4	IGAN-2265	1200 ± 100	690AD–950AD	1120 ± 100	Olsha	54.76897	31.84044	166.5	6.0	F	0.80–1.18	OB+BS	H		11	21		L	H	3
5	GIN-14374	1520 ± 280	140AD–780AD	1480 ± 300	Gn-10-05	54.77555	31.86911	169.0	8.5	F	8.00	OB	C		23			M		1
6	GIN-14370	10120 ± 70	10020BC–9550BC	11730 ± 170	Gn-10-02	54.77468	31.87012	170.5	10.0	T	4.00–4.30	Ch	M		33			H		1
7	GIN-14614	9460 ± 90	9120BC–8620BC	10770 ± 170	Gn-10-02	54.77468	31.87012	170.5	10.0	T	5.60–5.70	Ch	W		33			H		1
8	GIN-14615	21500 ± 650	24780BC–22990BC	25910 ± 890	GN-10-02	54.77468	31.87013	170.5	10.0	T	8.00	FB	W		15			L		1
9	IGAN-3311	920 ± 30	1040AD–1160AD	850 ± 40	GN-1-05	54.77807	31.86735	168.5	8.0	F	1.60–1.65	BS	H/B		11	21		L	M	1
10	IGAN-3331	1050 ± 50	890AD–1030AD	970 ± 60	GN-1-05	54.77807	31.86735	168.5	8.0	F	3.50–3.55	BP+CL	W		11			L		1
11	IGAN-3273	1160 ± 100	770AD–990AD	1090 ± 100	GN-1-05	54.77807	31.86735	168.5	8.0	F	4.45–4.60	BP	P		11			L		1
12	LU-5864	1130 ± 80	780AD–990AD	1060 ± 90	GN-18-07	54.77834	31.86766	165.5	5.0	F	1.00–1.05	Cl+BP, roof	W		11	21	M	L		1
13	GIN-14611	1580 ± 30	430AD–540AD	1470 ± 40	SV-1	54.77834	31.86766	165.5	5.0	F	1.80	BP	W		11			L		1
14	LU-6108	1260 ± 80	660AD–870AD	1170 ± 80	Proran-1	54.77784	31.86885	164.3	3.8	F	2.00	OB	W	21				M		1
15	IGAN-3943	760 ± 100	1150AD–1390AD	720 ± 90	GN-15-07	54.77785	31.86798	168.6	8.1	F	1.20	OB	C		31			H		1
16	IGAN-3829	390 ± 90	1440AD–1640AD	410 ± 90	GN-11-07	54.77762	31.86889	168.5	8.0	F	0.90–1.00	OB+BS	H/B		11	31		L	H	1
17	IGAN-3832	780 ± 70	1180AD–1290AD	730 ± 70	GN-11-07	54.77762	31.86889	168.5	8.0	F	1.07–1.17	OB+BS, foot	H/B	21	11		M	L		1
18	IGAN-2614	1040 ± 90	890AD–1150AD	960 ± 110	Bezdonka-1-02	54.77778	31.86966	164.5	4.0	F	0.70	BP, roof	P		11	31		L	H	4
19	IGAN-2615	760 ± 40	1220AD–1280AD	700 ± 30	Bezdonka-1-02	54.77778	31.86966	164.5	4.0	F	0.77	BP, roof	W		11	31		L	H	1
20	IGAN-2644	840 ± 40	1160AD–1260AD	760 ± 50	Bezdonka-1-02	54.77778	31.86966	164.5	4.0	F	1.10	BP, foot	P		11			L		1
21	IGAN-2645	1890 ± 30	60AD–140AD	1830 ± 40	Bezdonka-1-02	54.77778	31.86966	164.5	4.0	F	1.50	FB	H/B		21			M		4
22	IGAN-3750	500 ± 80	1310AD–1470AD	530 ± 80	N000W060	54.77813	31.87013	163.0	2.5	F	1.60–1.66	FB	H/B		21			M		1
23	IGAN-3751	820 ± 70	1150AD–1280AD	760 ± 70	N000W060	54.77813	31.87013	163.0	2.5	F	2.47–2.57	FB	H/B		21			M		1
24	IGAN-3309	750 ± 70	1200AD–1380AD	700 ± 70	N007W060	54.7782	31.87014	164.5	4.0	F	1.22–1.32	BP	P		11	21		L	M	1
25	IGAN-3317	1700 ± 90	220AD–510AD	1610 ± 110	N007W060	54.7782	31.87014	164.6	4.0	F	1.80–1.90	BP	P		21			L		1
26	IGAN-3727	450 ± 80	1400AD–1620AD	470 ± 80	S010W060	54.77804	31.87015	163.5	3.0	F	3.00–3.10	FB	P		11			L		1
27	IGAN-3752	110 ± 70	1680AD–1930AD	140 ± 90	S030W060	54.77787	31.87015	163.5	3.0	F	1.47–1.57	FB	P		21			L		1
28	IGAN-3729	640 ± 70	1280AD–1440AD	610 ± 50	S030W060	54.77787	31.87015	163.5	3.0	F	2.46–2.56	FB	P		21			L		1
29	IGAN-3310	750 ± 70	1200AD–1380AD	1250 ± 70	S040W060	54.77778	31.870146	164.5	4.0	F	1.17–1.25	BP	P		11	21		L	M	1

30	IGAN-3386	2360 ± 150	760BC–230BC	2430 ± 200	BD	54.77814	31.87108	165.3	5.0	F	4.00–4.30	OB	W	32	21		H	L		1
31	IGAN-2329	1590 ± 60	410AD–540AD	1480 ± 70	P-2-00	54.77836	31.87226	168.0	7.5	F	0.85	CL	W		11			L		1
32	IGAN-2328	1280 ± 50	670AD–780AD	1210 ± 60	P-2-00	54.77836	31.87226	168.0	7.5	F	1.00	CL	W		11			L		1
33	IGAN-2327	1870 ± 50	80AD–220AD	1800 ± 60	P-2-00	54.77836	31.87226	168.0	7.5	F	1.20	CL	W		11			L		1
34	IGAN-2325	1080 ± 90	780AD–1040AD	1010 ± 100	P-2-00	54.77836	31.87226	168.0	7.5	F	1.20	BP, roof	P		11	21		L	L	1
35	IGAN-2326	1330 ± 40	650AD–770AD	1250 ± 40	P-2-00	54.77836	31.87226	168.0	7.5	F	1.29	CL	W					L		1
36	IGAN-2435	1150 ± 50	780AD–970AD	1070 ± 70	P-2-01	54.77836	31.87226	168.0	7.5	F	0.80	CL	W		11			L		1
37	IGAN-2434	1290 ± 60	660AD–780AD	1210 ± 60	P-2-01	54.77836	31.87226	168.0	7.5	F	1.13	CL	W		11			L		1
38	IGAN-2436	1080 ± 70	880AD–1030AD	1010 ± 80	P-2-01	54.77836	31.87226	168.0	7.5	F	1.50	CL	W		11			L		1
39	IGAN-2437	1140 ± 40	830AD–980AD	1050 ± 60	P-2-01	54.77836	31.87226	168.0	7.5	F	1.50	CL	W		11			L		1
40	IGAN-2469	1220 ± 120	670AD–940AD	1130 ± 120	P-2-01	54.77836	31.87226	168.0	7.5	F	2.50	CL	H/B		11			L		1
41	IGAN-2471	1180 ± 70	770AD–970AD	1110 ± 80	P-2-01	54.77836	31.87226	168.0	7.5	F	2.50	CL	H/B		11			L		1
42	IGAN-2628	1140 ± 40	830AD–980AD	1050 ± 60	P-8-02	54.77776	31.87249	169.0	8.5	F	1.2	CL	C		11			L		1
43	IGAN-2646	1130 ± 30	880AD–980AD	1030 ± 40	P-8-02	54.77776	31.87249	169.0	8.5	F	1.2	CL	C		11			L		1
44	IGAN-2639	950 ± 60	1020AD–1160AD	850 ± 60	P-8-02	54.77776	31.87249	169.0	8.5	F	1.2	CL	H/B		11			L		1
45	IGAN-3833	870 ± 60	1040AD–1230AD	800 ± 70	P-8-07	54.77781	31.87213	168.4	7.9	F	1.20–1.30	OB+CL	H/B	21				M		1
46	LU-6297	540 ± 110	1290AD–1450AD	550 ± 90	DP-2-09	54.77697	31.87223	168.5	8.0	F	0.80–0.90	OB	C		31			H		1
47	GIN-14377	1050 ± 200	770AD–1170AD	990 ± 190	DP-2-10	54.7768	31.87205	168.5	8.0	F	2.40–2.50	OB	C		21			M		1
48	LU-5983	470 ± 60	1390AD–1490AD	500 ± 70	S040E120	54.77778	31.87297	167.5	7.0	F	1.70–1.80	BP	P		11	31		L	H	1
49	IGAN-3744	790 ± 60	1180AD–1280AD	730 ± 60	S040E120	54.77778	31.87297	167.5	7.0	F	2.40–2.53	BP	P	21	11		L	L		1
50	LU-5984	960 ± 70	1020AD–1160AD	860 ± 70	S040E120	54.77778	31.87297	167.5	7.0	F	2.80–2.92	BP	P		21	11		L	L	1
51	IGAN-3753	380 ± 60	1440AD–1630AD	410 ± 60	S040E140	54.77778	31.87327	167.5	7.0	F	1.94–2.06	BP	P		11	31		L	H	1
52	IGAN-3276	360 ± 50	1460AD–1630AD	410 ± 60	S060E120	54.77758	31.87297	167.5	7.0	F	1.90–2.00	FB+BP	P		11	31		L	H	1
53	IGAN-3325	1390 ± 90	560AD–770AD	1300 ± 90	S060E120	54.77758	31.87297	167.5	7.0	F	2.75–2.85	FB+BP	W		11		L	L		1
54	IGAN-3733	340 ± 90	1470AD–1640AD	370 ± 110	S020E120	54.77796	31.87327	167.5	7.0	F	1.95–2.05	BP	P		11			L		1
55	IGAN-3745	80 ± 60	1690AD–1920AD	130 ± 80	S020E140	54.77796	31.87327	167.5	7.0	F	1.80–1.90	BP	P		11			L		1
56	IGAN-3732	620 ± 70	1290AD–1400AD	600 ± 40	S020E140	54.77796	31.87327	167.5	7.0	F	2.60–2.70	BP	P		11			L		1
57	LuS-8147	555 ± 120	1280AD–1450AD	560 ± 100	S031E138	54.77787	31.87324	167.5	7.0	F	1.47–1.48	FB	W		31			H		1
58	LuS-8790	425 ± 50	1420AD–1620AD	450 ± 60	S031E138	54.77787	31.87324	167.5	7.0	F	1.47–1.48	FB	W		31			H		1
59	LU-5985	550 ± 60	1310AD–1440AD	580 ± 50	S031E138	54.77787	31.87324	167.5	7.0	F	2.15–2.20	BP	P		11	31		L	H	1
60	LU-5986	1120 ± 60	820AD–1000AD	1040 ± 70	S031E138	54.77787	31.87324	167.5	7.0	F	2.70–2.80	BP	P	21	11			L		1
61	IGAN-3830	1680 ± 80	240AD–510AD	1590 ± 100	S031E138	54.77787	31.87324	167.5	7.0	F	3.80–3.90	BP	P		21			L		1
62	IGAN-3834	1440 ± 60	560AD–660AD	1350 ± 50	S031E138	54.77787	31.87324	167.5	7.0	F	3.35–3.45	BP	P		21			L		1
63	LuS-8788	1895 ± 50	50AD–210AD	1830 ± 60	S031E138	54.77787	31.87324	167.5	7.0	F	4.99	FB	W		21			L		1
64	IGAN-1801	1240 ± 100	680AD–890AD	1150 ± 100	Sedov	54.77831	31.87317	168.5	8.0	F	1.2	CL	H/B		11	21		L		1
65	IGAN-1826	1300 ± 60	660AD–780AD	1220 ± 60	Sedov	54.77831	31.87317	168.5	8.0	F	1.2	CL	C		11	21		L		1
66	IGAN-1804	1120 ± 120	770AD–1030AD	1050 ± 130	P-4	54.77831	31.87317	168.5	8.0	F	1.40–1.45	CL+OB, roof	W		11	21		L		1
67	Ki-13989	2250 ± 150	510BC–50BC	2280 ± 200	N017E160	54.77829	31.87359	169.3	9.0	F	1.20–1.30	OB	W	32	21		H	L		1
68	GIN-14687	1750 ± 250	1AD–560AD	1710 ± 280	GN-11-10	54.77554	31.87246	168.0	7.5	F	12.00–13.00	FB	W		23			M		1
69	GIN-14613	780 ± 40	1220AD–1280AD	710 ± 30	GN-11-02	54.77572	31.87270	168.0	7.5	F	7.40–7.50	FB	W		23			M		1
70	LU-5869	910 ± 80	1030AD–1190AD	830 ± 70	GN-5-07	54.77568	31.87273	168.5	8.0	F	2.56	OB	C		21			M		1
71	IGAN-3835	6540 ± 70	5620BC–5390BC	7450 ± 70	GN-3-07	54.77653	31.87418	169.2	8.5	F	2.63–2.70	OB+BS	H/B		11	21		L	M	1
72	LuS-8145	245 ± 100	1490AD–1960AD	260 ± 140	GN-1-07	54.77723	31.87573	170.0	9.5	F	1.50	OB	C		31			H		1
73	IGAN-3705	1260 ± 60	670AD–860AD	1180 ± 70	GN-1-07	54.77723	31.87573	168.3	8.0	F	2.65–2.68	OB	H/B		11	21		L	M	1
74	LU-5865	1350 ± 70	610AD–770AD	1260 ± 70	GN-1-07	54.77723	31.87573	168.3	8.0	F	2.77–2.79	OB	W		11			L		1
75	LU-6076	1250 ± 60	680AD–860AD	1170 ± 70	GN-1-07	54.77723	31.87573	168.3	8.0	F	2.99–3.09	CL	W		11			L		1

76	LU-5866	1200 ± 80	700AD–940AD	1120 ± 90	GN-1-07	54.77723	31.87573	168.3	8.0	F	2.99–3.09	OB+CL	W		11			L		1
77	IGAN-3706	1850 ± 40	120AD–230AD	1780 ± 50	GN-1-07	54.77723	31.87573	168.3	8.0	F	3.18–3.20	OB+Bp	W		11			L		1
78	LU-5867	1870 ± 70	70AD–240AD	1800 ± 80	GN-1-07	54.77723	31.87573	168.3	8.0	F	3.20–3.23	OB	P		11			L		1
79	IGAN-3728	1340 ± 70	630AD–780AD	1250 ± 70	GN-1-07	54.77723	31.87573	168.3	8.0	F	3.58–3.60	BP	P		11			L		1
80	LU-5868	2100 ± 60	200BC–40BC	2090 ± 90	GN-1-07	54.77723	31.87573	168.3	8.0	F	3.75–3.78	OB	P		11			L		1
81	LU-5862	2370 ± 80	750BC–370BC	2460 ± 140	GN-1-07	54.77723	31.87573	168.3	8.0	F	5.00–5.10	Ch	W	32	11		H	L		1
82	GIN-11522	1530 ± 40	430AD–600AD	1430 ± 50	RAZ-1	54.77709	31.87538	168.2	8.0	F	3.10–3.30	OB	W		11			L		2
83	GIN-11523	2230 ± 40	380BC–210BC	2240 ± 60	RAZ-1	54.77709	31.87538	168.2	8.0	F	6.00	FB	W	32	21		H	L		2
84	GIN-11959	1200 ± 100	690AD–950AD	1120 ± 100	RAZ-3	54.7766	31.87429	169.0	8.5	F	2.65	OB	C		21			L		2
85	GIN-11523a	550 ± 100	1290AD–1450AD	560 ± 80	RAZ-4	54.77734	31.87587	168.5	8.0	F	2.20–2.48	OB	C		21	31		M	H	2
86	GIN-11958	1330 ± 30	650AD–770AD	1260 ± 40	RAZ-7	54.77721	31.87568	168.3	8.0	F	3.20–3.30	OB	W		11			L		2
87	IGAN-3590	1820 ± 70	80AD–320AD	1750 ± 90	STAR-1	54.77305	31.88259	164.1	3.6	FP	3.60–4.60	FB	M	34	21		H	L		1
88	IGAN-3582	2030 ± 60	120BC–60AD	2000 ± 80	STAR-2	54.77305	31.88259	164.1	3.6	FP	3.30–3.90	FB	M	34	21		H	L		1
89	IGAN-3847	170 ± 60	1660AD–1960AD	160 ± 90	LB-1-07	54.77386	31.89063	169.9	9.0	F	0.59–0.62	OB+BS, roof	H/B		11	21		L	M	1
90	IGAN-3837	310 ± 70	1490AD–1650AD	360 ± 100	LB-1-07	54.77386	31.89063	169.9	9.0	F	0.95–0.98	OB+BS, foot	H/B	21	11		H	L		1
91	IGAN-3891	5200 ± 130	4240BC–3810BC	5980 ± 160	LB-1-07	54.77386	31.89063	169.9	9.0	F	2.02–2.06	OB+BS, roof	H/B		11	21		L	M	1
92	IGAN-3890	2120 ± 110	360BC–1BC	2110 ± 140	GN-4-08	54.77261	31.89075	163.9	3.2	FP	6.00–6.30	FB	M	34	21		H	L		1
93	LU-5988	1980 ± 70	60BC–130AD	1940 ± 90	GN-6-08	54.77227	31.89084	163.9	3.2	FP	5.57–5.68	FB	M	34	21		H	L		1
94	IGAN-3719	3120 ± 120	1530BC–1210BC	3320 ± 150	GN-1-08	54.7831	31.91390	164.0	3.0	FP	3.63–3.66	FB	W	12	12		L	L		1
95	LU-5982	3190 ± 350	1900BC–1000BC	3460 ± 450	GN-1-08	54.7831	31.91390	164.0	3.0	FP	4.47	FB	C	12	12		L	L		1
River Katynka																				
96	IGAN-3378	3980 ± 70	2620BC–2340BC	4450 ± 120	KAT-2a	54.76561	31.70670	167.5	7.5	F	3.80–4.10	FB	H/B	34			H			1
97	IGAN-3911	3130 ± 90	1510BC–1290BC	3340 ± 110	KAT-3-07	54.76822	31.71061	167.5	5.8	F	6.10–6.25	OB	W		21			M		1
98	IGAN-3277	1380 ± 100	560AD–780AD	1290 ± 100	KAT-3a	54.76587	31.70504	169.0	9.0	F	0.60–0.70	BS, roof	H/B		11	31		L	H	1
99	IGAN-3324	5170 ± 130	4230BC–3790BC	5940 ± 160	KAT-3a	54.76587	31.70504	168.5	8.5	F	4.50–4.80	FB	W	34			H			1
100	IGAN-3945	2290 ± 130	710BC–170BC	2330 ± 190	KAT-8-07	54.76906	31.71351	167.1	4.8	F	5.85–5.90	Ch	W		23			M		1
101	LU-5861	370 ± 80	1440AD–1640AD	400 ± 80	KAT-9-07	54.76882	31.71314	164.3	2.0	F	1.38	Ch	W		21			M		1
102	IGAN-3831	830 ± 70	1050AD–1280AD	770 ± 70	KAT-10-07	54.78192	31.71562	166.0	1.7	F	0.34–0.39	OB+BS, roof	H/B					L	H	1
103	IGAN-3836	2070 ± 80	200BC–20AD	2060 ± 110	KAT-10-07	54.78192	31.71562	166.0	1.7	F	0.58–0.63	OB+BS, foot	H/B				H	L		1
104	IGAN-3749	5890 ± 100	4910BC–4610BC	6720 ± 130	KAT-11-07	54.78257	31.71595	164.7	0.5	F	2.17–2.27	OB	H/B		11			L	H	1
River Vop'																				
105	Ki-13987	100 ± 80	1680AD–1940AD	140 ± 90	VOP-1	55.19460	32.84139	179.0	2.5	F	1.80–1.90	OB, foot	W	36	23		H	M		1
River Khmost'																				
106	Ki-13988	2790 ± 90	1050BC–830BC	2930 ± 110	HM-1	54.87729	32.46031	182.5	3.5	F	3.40	Ch	W		21			M		1
107	Ki-13990	960 ± 100	990AD–1190AD	870 ± 100	HM-3a	54.87744	32.46068	181.0	2.2	F	2.20–2.30	FB, foot	W	34			H			1
108	IGAN-3306	840 ± 70	1050AD–1270AD	780 ± 70	HM-4	54.87763	32.461297	183.0	4.1	F	0.45 (0.50)	OB	C		31			H		1
109	IGAN-3725	2510 ± 60	790BC–540BC	2580 ± 100	HM-4	54.87763	32.461297	183.0	4.1	F	0.58–0.70	OB	H/B	31			H			1
110	IGAN-3380	2800 ± 170	1220BC–800BC	2960 ± 210	HM-4	54.87763	32.461297	183.0	4.1	F	0.95 (0.97)	OB	C		31			H		1

Table 2. *OSL dates from the upper Dnieper River valley.*

					Core/section location						Sample characteristics		Fluvial events[4]		Fluvial activity class[5]		
No.	**Index (GdTL)**	**Date (cal yrs BP)**	**Equivalent dose (Gy)**	**Effective dose rate (Gy/ka)**	**Name**	**Latitude (°N)**	**Longitude (°E)**	**Absolute height (m)**	**Elevation above the river (m)**	**Geomorphology[1]**	**Depth (m)**	**Stratigraphy[2]**	**post-dated**	**dated**	**post-dated**	**dated**	**Source[6]**
1	1465	7160 ± 620	13.20 ± 0.10	1.826 ± 0.68	Ch-11-02	54.7578	31.7316	170	10	TP	3.00-3.50	Ch		33		H	1
2	1466	8690 ± 570	13.93 ± 0.75	1.591 ± 0.57	Ch-11-04	54.7598	31.7241	187	27	ER	1.40	Ae		38		H	1
3	1467	8200 ± 440	15.77 ± 0.61	1.908 ± 0.67	Ch-11-05	54.7617	31.7138	175	15	T	1.60-2.00	Ch		33		H	1
4	1239	4690 ± 700	7.90 ± 0.11	1.653 ± 0.68	Gn- 10-24	54.7553	31.7324	173	13	T	1.60	SW		37		H	1
5	1238	21400 ± 280	19.30 ± 0.23	0.896 ± 0.42	Gn-10-02	54.7747	31.8701	170.5	10	T	9.40	FB		15		L	1
6	1235	1140 ± 140	2.71 ± 0.28	2.248 ± 0.91	Dp-2/2010	54.7768	31.8721	168.5	8	F	1.40	OB		31		H	1
7	1237	780 ± 60	2.43 ± 0.13	2.89 ± 0.11	P-8/2010	54.7778	31.8721	168.5	8	F	1.00	OB	11	31	L	H	1
8	1236	590 ± 60	1.66 ± 0.14	2.525 ± 0.99	P-8/2010	54.7778	31.8721	168	7.5	F	0.37	OB		31		H	1
9	1470	11020 ± 830	17.50 ± 0.11	1.578 ± 0.66	Kor-11-02	54.9250	32.7230	176	9	T	3.20-3.60	Ch		33		H	1
10	1468	10050 ± 670	17.37 ± 0.96	1.718 ± 0.62	Kor -11-05	54.9166	32.7422	195	28	ER	1.40-1.45	Ae		38		H	1
11	1469	8850 ± 670	19.10 ± 0.13	2.141 ± 0.76	Kor-11-06	54.9114	32.7679	172	5	FP	1.60-1.65	Ch		33		H	1

Dates are grouped in the downstream — upstream order.

Notes to Tables 1–2:

[1] *F — floodplain, FP — floodplain palaeochannel, T — terrace (low), TP — palaeochannel on low terrace; ER — erosion remnant*

[2] *Ch — channel alluvium, OB — overbank alluvium, FB — sediments from floodplain basins (oxbows, lakes, etc.), BS — buried soil, BP — buried peat, CL — cultural layers at archaeological sites, SW — slopewash deposits, Ae — aeolian cover sands*

[3] *W — wood, C — charcoal, P — peat, M — macrofossils, H/B — humic acids/bulk*

[4] *Fluvial and related events:*

1. Low activity events: 11 — no sedimentation on high floodplain levels (soil formation, accumulation of peat), weak sedimentation on low levels; 12 — small palaeochannels, 13 — channel type characteristic for lower discharges; 14 — aeolian activity on sandy terraces that indicates dry conditions; 15 — river damming.

2. Medium activity events: 21 — usual overbank and basin sedimentation; 22 — palaeochannels of modern type and size; 31 — lateral river migrations of modern rate an type.

3. High activity: 31 — active overbank sedimentation on high floodplain levels (coarser grainsize, distinct lamination), 32 — erosion of floodplain surface by flood flows; 33 — large palaeochannels; 34 — chute cutoffs; 35 — channel type characteristic for higher discharges; 36 — type and rate of lateral river migrations characteristic for higher discharges; 37 — active slopewash on valley sides; 38 — aeolian activity that indicates existence of wide channels with extensive sandbars.

[5] *L — low, M — medium (similar to present-day), H — high.*

[6] *1 — this study, 2 — Aleksandrovskiy* et.al.*, 2005, 3 — Bronnikova* et.al.*, 2003, 4 — Bronnikova and Uspenskaya, 2007.*

We accounted also for indirect features such as:

d) sand covers blown from the valley from wide alluvial plains formed due to migration of large channels.

e) active slopewash on valley sides;

For each date its concurrence, pre-dating and post-dating of corresponding events was also indicated (see **Tables 1**, **2**). A given date is regarded as concurrent to a fluvial event that produced the dated sedimentary unit. In addition, dates from basal part of a sedimentary unit may also post-date an event that preceded the unit formation. For example, a date from the base of a palaeochannel infill is a post-date for an avulsion event. A date from the top part of a sedimentary unit may also pre-date an event that followed the unit formation. For example, the top of a buried floodplain soil or peat predates the sedimentation event that has buried it. The time offset between ages of the dated sediment and desirable event is usually unknown and may reach several centuries, which should be taken into account while interpreting bracketing dates, particularly at centennial time scale.

Stage 3. Producing integral probability density functions.

The high, medium and low activity sets of dates were treated using the Sum function of the OxCal program, version 4.2 [74] (Bronk Ramsey, 2009) with the IntCal'09 calibration curve (Reimer *et al.*, 2009). For the high activity class we analyzed also bracketing dates: those that post-date fluvial events and make their younger constraints, and those pre-dating events and making their older constraints.

The form of the Probability Density Function (PDF) is determined by three arguments: (1) frequency distribution of studied events, (2) the young age bias — rising trend of date frequency in with decreasing age that comes from better preservation of younger sediments and landforms, (3) the form of calibration curve. Of them only the first one represents the wanted signal while the two latter factors make statistical noise. To account for the form of calibration curve Lewin *et al.* (2005) suggested constructing a synthetic regularly spaces data set and subtracting its PDF from the PDF of real data. Hoffmann *et al.* (2008) proposed normalization of PDF for each data group through dividing it by PDF of the complete data set. This procedure permits to eliminate not only the effect of wiggles of the calibration curve, but also the young age bias.

The application of correcting procedures makes sense at time intervals with continuous coverage by computed PDF. Our data set is characterized by repeated gaps beyond the Late Holocene (**Fig. 3**). Therefore we apply the correction proposed by Hoffmann *et al.* (2008) for the time span 3.0–0 ka only. To do that the summed PDFs for each group were divided by the total data set PDF (**Fig. 3**) to obtain relative PDFs (RPDF). RPDF were calculated for the whole time interval but were analyzed only for the last 3 ka.

The PDFs were computed for three classes of fluvial activity (low — LA, medium — MA, high activity — HA) using the respective groups of concurrent dates. OSL and uncalibrated radiocarbon dates were put together in combined data sets using the C_Date and R_Date functions of OxCal. OSL dates were calculated with respect to AD1950, and option "Use BC/AD not BP" was switched to "False". For the high activity class PDFs of the two groups of bracketing dates (pre-dates and post-dates) were also constructed.

All ages in the text are presented in calibrated years before present (cal BP) where 0 cal BP corresponds to AD 1950.

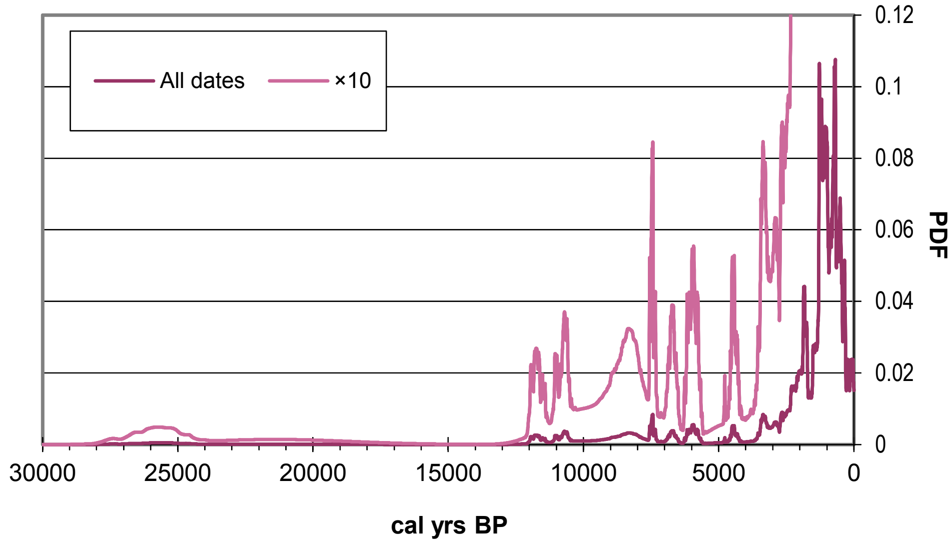

Fig. 3. *Probability density function (PDF) of all dates. Note: pre-Holocene time is supplied with only one OSL date 21400 ± 280 (no.5 in Table 2) obtained from sedimentary units at the base of the Late Glacial – Early Holocene terrace interpreted as sediments of the glacial-dammed lake.*

4. RESULTS

There are only two pre-Holocene dates in the data set (no.8 in **Table 1**, no.5 in **Table 2**) that produce a slight rise of PDF in the interval 27–20 ka cal BP (**Fig. 3**). Both dates were attributed to the low activity class. They were obtained from aquatic silts and clays found at the base of low river terrace downstream from Smolensk. These deposits were also found by coring under the Holocene floodplain and present-day point-bars, *i.e.* widely across the valley bottom. Within the generally fine sediments lenses of coarse sand are found evidencing existence of periodical flows in shallow channels probably of braiding or anastomosing type. The sedimentary environment looks like a semi-closed periodically (seasonally?) drained-out lake established in the valley around LGM.

The interval between LGM and the beginning of the Holocene is not characterized by any absolute dating. For the Early Holocene in the interval 12–7.5 ka cal BP, characteristic is high fluvial activity (**Fig. 4c**). It is supported by dates from large palaeochannels and attendant phenomena (aeolian sand transport from wide alluvial plains) in the Dnieper valley (**Table 2** — no.1–3 and 9–11). The younger boundary of this epoch is constrained by low-activity dates at 7.5–6 ka cal BP (**Fig. 4a**). The extending high-activity epoch into ages younger than 8 ka cal BP is supported only by the OSL date 7160 ± 620 from alluvium of the large palaeochannel at the Chekulino village (no. 1 in **Table 2**; **Fig. 2**). The radiocarbon date 8330 ± 350 (no.1 in **Table 1**) from the base of the peat deposits that cover the same palaeochannel and post-date its activity evidences that the above OSL date is too young. Therefore the younger boundary of this high-activity epoch has been shifted to 8 ka cal BP. Individual peaks within the high-activity epoch reflect rather a deficit of data (some 10 dates for the >4-ka period) than any internal variations of fluvial activity. We do admit that this epoch may not be homogeneous, but the small amount of collected data is not sufficient to sub-divide it.

In the period 7.5–6 ka cal BP, several well developed forest-type soils were dated in the floodplains indicating low flood activity (**Fig. 4a**; **Table 1** — no.71, 91, 104). No alluvial sediments have been dated from the interval between 6–4 ka cal BP, which evidences indirectly that the low activity epoch had still been going on. It was interrupted by high activity episodes between 6.0–6.5 and <4.4 ka cal BP (**Fig. 4c**). These high activity events were found only in tributary valleys (**Table 1** — no.99, 96). The latter episode may be correlated to the active slope-wash event at the Dnieper valley side dated around 4.7 ka cal BP (**Table 2** — no.4). Since 4 ka cal BP the total number of dates increases considerably. Till 3 ka cal BP, prevailing are low- and medium-activity dates. Therefore the interval 7.5–3 ka cal BP may be in general considered as a low fluvial activity epoch with short lasted breaks by high activity episodes that exhibited mostly in tributary valleys of small rivers.

The interval since 3 ka cal BP till present is characterized by occurrence of all activity classes (**Fig. 5**). Sometimes they follow each other, in other cases they overlap, which demand additional comments. For this interval we use relative PDFs (normalized to the total data set) that show a clearer picture than the initial sum of PDFs. The number of dates is sufficient for the designation of some centennial rhythms of fluvial activity.

The first episode of high activity is detected between 2.7 and 3.0 ka. It starts with a decline of the LA PDF and rise of the HA PDF at 3.2–3.0 ka cal BP and ends with a drop of HA RPDF with a concurrent sharp rise of the HA post-date PDF and LA PDF at ~2.7 ka cal BP (**Fig. 5a**, **5c**). A change to more active fluvial development in this interval is illustrated also by the peak of MA RPDF (**Fig. 5b**) which almost mirrors the trough of the LA curve. On the other hand, this MA maximum shows that the activity was not too high.

The period 2.7–1.8 ka cal BP is marked by a prominent flat-topped peak of the HA post-date RPDF **Fig. 5c**). Its big width evokes doubt that the peak may be totally attributed to the preceding 3.0–2.7 ka rise of HA. All the HA post-dates refer to the base of the sedimentary infill of palaeochannels or ancient flood erosion forms on floodplains in both, Dnieper and its tributary, valleys (**Table 1** — nos. 30, 67, 81, 83, 87, 88, 92, 93, 103, 109). The time offset between the age of the lower units of infill and an extreme event responsible for channel chute cutoff or boring large erosion pots on floodplain, may be from several decades to a few centuries, not 700–900 years. Therefore most probably the right (younger) part of the HA post-date peak indicates a separate HA episode, or the sequel of the 3.0–2.7 ka rise, which is not characterized by concurrent dates. Indicative is also the form of LA RPDF with relatively low values around 2.5–2.6 ka and rising trend till 2.3–2.0 ka (**Fig. 5a**). To a large extent the LA and post-date HA RPDFs are produced here in a big part by the common set of dates: many dates are marked concurrent to LA conditions but post-date HA events. Given that, we infer that the interval about 2.3–2.7 ka cal BP should be designated as an HA episode. In total, the HA phase is limited to 3.0–2.3 ka cal BP. Given the number of dates and geomorphic objects evidencing extreme events, the second half of this interval (2.3–2.7 ka cal BP) was probably characterized by the highest activity.

The subsequent interval of low activity is best exhibited by the LA RPDF that peaks between 2.3–0.9 ka cal BP (**Fig. 5a**). A drop of LA RPDF between 1.0–0.9 ka cal BP corresponds to the initial rise of HA which peaks at 0.6–0.5 ka cal BP (**Fig. 5c**). The whole interval 0.9–0 ka cal BP is characterized by the presence of all activity classes. Most LA dates are taken from the bases and tops of buried organic horizons and both indicate concurrent low flooding and post-date or pre-date high flooding episodes with active mineral sedimentation on floodplains. Therefore in spite of the major contribution from

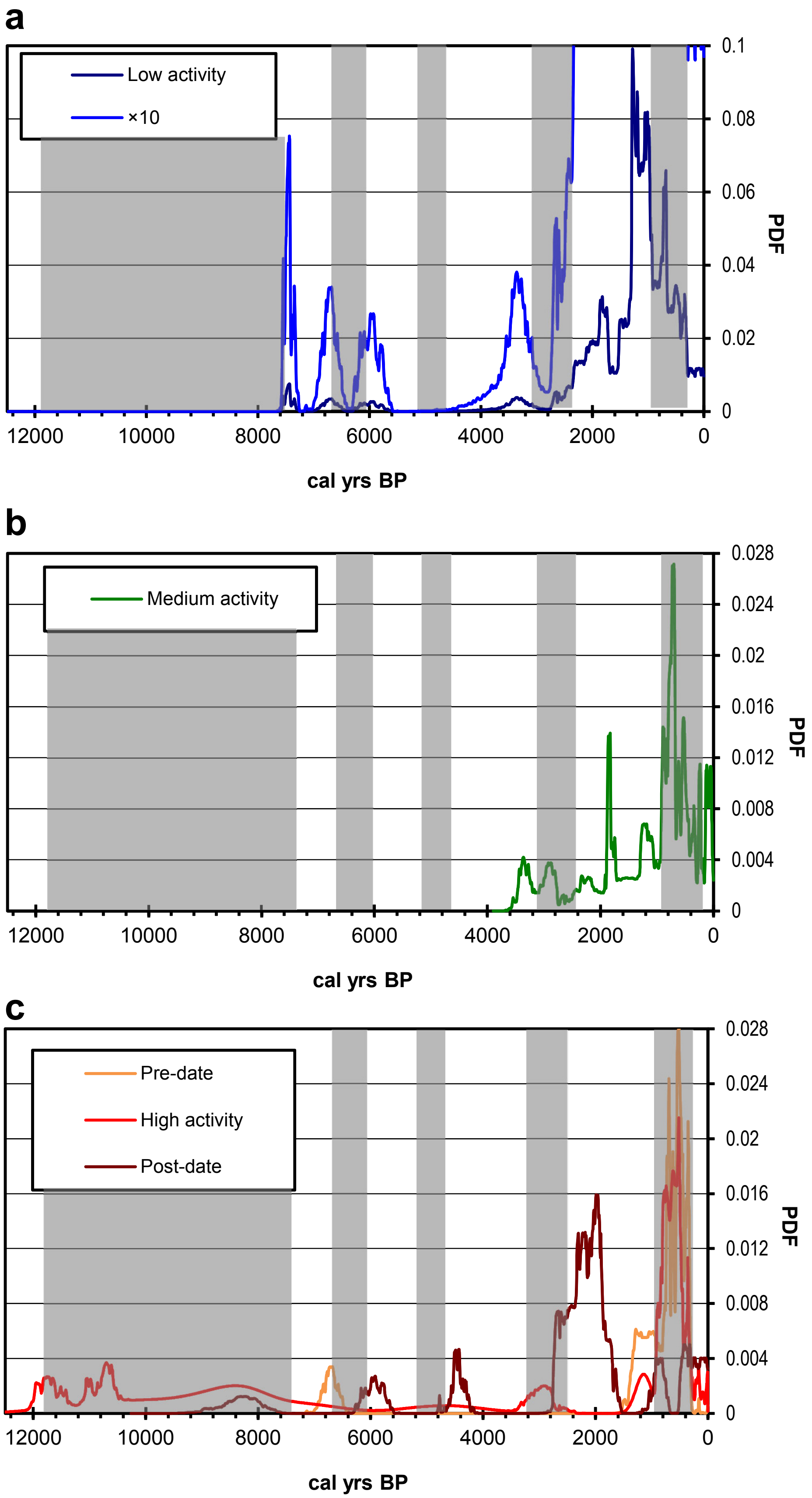

Fig. 4. *The Holocene coverage of probability density functions (PDF) of dates from different fluvial activity classes: a — low activity, b — medium activity, c — high activity. Light-grey strips are intervals of high fluvial activity. Time scale starts in 1950AD.*

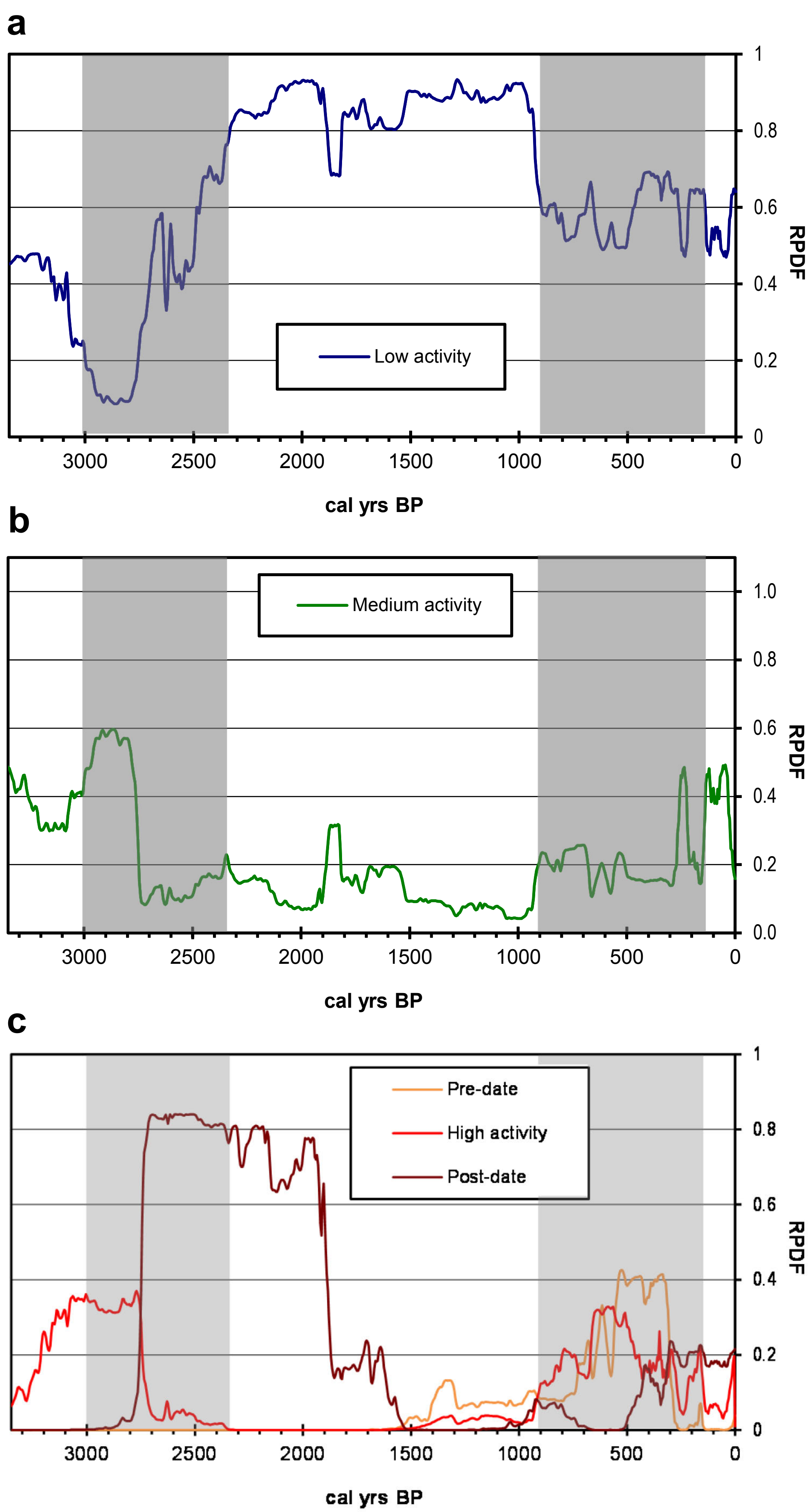

Fig. 5. *The Late Holocene coverage of relative probability density functions (RPDF) of dates from different fluvial activity classes: a — low activity, b — medium activity, c — high activity. Light-grey strips are intervals of high fluvial activity. Time scale starts in 1950AD.*

the LA class, we consider this picture as exhibition of irregular chronological structure — alternation of decadal to centennial episodes of high and moderate to low flooding. High flooding intervals may be best drawn from concurrent, pre-dating and post-dating HA RPDF (**Fig. 5c**): 0.9–0.5 ka cal BP (mid-11–mid-15th c.) with the most active phase at 0.6–0.5 ka cal BP (mid-14–mid-15th c.), and 0.3–0.1 ka cal BP (mid-17 –mid-19th c.). Obtaining more exact constraints for historical hydrological epochs is not possible because of limited accuracy of radiometric methods.

5. DISCUSSION AND FINAL REMARKS

The findings on the lacustrine environments occurring in the Dnieper valley around LGM contribute to the long-lasting discussion on the ice sheet boundary at its maximal stage and its influence on the Dnieper River. The northernmost part of the Dnieper catchment was covered by the Valdaian (Weichselian) glaciation around the Last Glacial Maximum (LGM), but the exact position of the LGM ice-sheet boundary is steel debatable. On maps released by Russian Geological Survey the LGM glacial boundary is shown northwards from the Dnieper valley (Stolyarova, 1970; Barashkova *et al.*, 1998). A possible crossing of the Dnieper valley by the Late Valdaian ice sheet proposed by Salov (1972) gave rise to the hypothesis of the Smolensk-Dorogobuzh, or Dnieper, glacial dammed lake that was thought to have overflowed into the Oka-Volga basin and contributed the Pleistocene-highest level rise of the Caspian sea — the Khvalyn' transgression (Kvasov, 1979).

The lacustrine sediments near Smolensk dated to around the LGM support the idea of the ice sheet reaching the valley and promoting formation of the glacial-dammed lake. On the other hand, maximal elevation of lacustrine sediments found at Smolensk does not exceed 170 m a.s.l. Traces of flow — sand lenses within the lacustrine fines — speak against the existence of big depths in this lake. Therefore the lake level could not rise to 215 m abs, which according to Kvasov (1979) was necessary for the lake water to have overflowed into the Volga Basin.

The glacial melt water output is regarded as an important governing factor for the post-LGM level changes of the Black Sea (Lericolais *et al.*, 2011; Sidorchuk *et al.*, 2011). Large pulses of glacial-melt waters delivered to the Black Sea have been interpreted from geochemical composition of bottom sediments in the north-western shelf and dated to 18–16 ka cal BP (Major *et al.*, 2006). Traces of this transportation of huge amounts of water were thought to be extremely large braiding palaeochannels of Dnieper found in the Russian and Byelorussian sections of the river from the confluence with the Vop' River downstream to the Rogachov city. Wide and long abandoned channels separated from the modern river by moraine hills similar to that found in the Upper Dnieper (see **Fig. 2**) were interpreted in the Byelorussian part of the valley as dead valley branches formed by glacial-fed high-discharge river and abandoned after the glacial water inflow had ceased (Kalicki and Sańko, 1992, 1998). Based on specific morphology of these palaeochannels, Kalicki (1995) suggested the new type of disparity between the present-day river and its valley bottom — the Dnieper type of river underfitness.

Glacio-fluvial explanation of the traces of large water flows through the Dnieper valley should now be questioned by the Early Holocene ages (9–7 ka cal BP) of two large palaeochannels presented in this paper. Channel sands from two different palaeochannels at the Chekulino and Korovniki villages were dated by OSL and gave 7160 ± 620 years (no.1 in **Table 2**) and 8850 ± 670 years (no.11 in **Table 2**), respectively. The former (downstream) palaeochannel surface is 10 m above the river and thus relates to the low terrace level, and the latter (upstream) one lies only 5 m above the river and is subject to inundation by spring floods along with the modern floodplain (**Table 2**); these differences are probably due to glacioisostatic crustal movements (forebulge rebound). The date 8200 ± 440 years (no.3 in **Table 2**) gives the age of the low terrace at the opposite side of the high erosion remnant (**Fig. 2**) and indicates the moment of channel avulsion through the relic moraine hill. This avulsion must have been conditioned by high flood stages of the river so that the stream could overflow the hill at its lowest site.

Aeolian sands on top of erosion remnants alongside the large palaeochannel were dated to 8690 ± 570 and 10050 ± 670 years respectively (no.2 and 10 in **Table 2**). We suppose that aeolian activity in Early Holocene had local character and was maintained by existence of vast bare sand areas in the close vicinity. With respect to confidence intervals, proximity of dates on aeolian sands and alluvial sands from nearby large palaeochannels support that there may have been bars of these palaeochannels to supply sand for aeolian covers. If so dates on aeolian sands indirectly support the Early Holocene formation of large palaeochannels. Another support is from the radiocarbon date 8330 ± 350 cal BP (no.1 in **Table 1**) derived from the base of the peat lens inset into the palaeochannel whose accumulation must have started shortly after the alluvial activity in the palaeochannel was finished.

The Early Holocene age estimations of the large palaeochannels in the Upper Dnieper imply that formation of these palaeochannels was rather a climatic than glacio-fluvial phenomenon and high river runoff that produced these channels had meteoric origin and was climatically driven. It brings up the question of chronology of the high river runoff epoch in Central and Eastern Europe. In the central part of the East European Plain large meandering palaeochannels (macromeanders) were dated between 18 and 13 ka cal BP (Borisova *et al.*, 2006; Sidorchuk *et al.*, 2009). Active development or abandonment of large meanders in various regions of Central Europe were dated to different but in all cases to pre-Holocene times in the range 16–12 ka cal BP: since the Bølling till the end of Younger Dryas in Poland (Szumanski, 1983, 1986; Vandenberghe *et al.*, 1994; Gębica *et al.*, 2009) and Hungary (Kasse *et al.*, 2010), about 15.5 ka cal BP (12.8 ka ^{14}C BP) in the Lower Danube region (Howard *et al.*, 2004). In southern Poland some rivers did not change their pattern from braiding to large meanders during the Late Glacial and kept braiding to the beginning of the Holocene (Starkel *et al.*, 1996; Gębica, 2011), other rivers transformed from meandering back to braiding in the Younger Dryas (Starkel and Gębica, 1995), but in all cases the Late Glacial phase of increased fluvial had declined almost exactly at the Younger Dryas / Holocene transition (Gębica, 2013).

The Upper Dnieper exhibits the only case of large palaeochannels in Europe to have been dated to the Early Holocene. Both in Poland (Gębica, 2013) and in the European part of Russia (Borisova *et al*., 2006; Sidorchuk *et al*., 2012) dated to this time were small palaeochannels whose sizes and consequently river channel-forming discharges were similar to that of present-day rivers. On the other hand, continuation of high runoff from the Late Glacial into the first half of the Holocene has been found in some parts of North America: large river meanders were dated to 12–9.5 ka cal BP in the Great Lakes region (Arbogast *et al.*, 2008) and to 15–5 ka cal BP in the Southeastern USA (Leigh, 2006). It demonstrates principal possibility of large palaeochannel formation in the Holocene, though it has not yet been known in Europe.

The evidence of high runoff production by the Upper Dnieper in the Early Holocene contributes to better understanding the post-glacial level change of the Black Sea which receives the Dnieper's waters. According to Lericolais *et al.* (2010), in the period 13.0–9.5 ka cal BP (11.0–8.5 ka ^{14}C BP) the Black Sea exhibited regression and low stand, which was followed by rapid ultimate transgression starting immediately after ~9.5 ka cal BP (8.5 ka ^{14}C BP). According to our results, the Upper Dnieper River had high discharges since the very beginning of the Holocene till about 8 ka cal BP. Therefore it makes unlikely the Black Sea to have kept low stage in the Early Holocene. Even if this lowstand had been really occurring, it could hardly be governed by river runoff decrease as it was proposed in (Lericolais *et al.*, 2010).

The Mid-Holocene at the Upper Dnieper was marked by dominating low fluvial activity at 8–3 ka cal BP marked by formation of zonal-type soils on floodplains, with short episodes of high floods occurred between 6.5–4.4 ka cal BP. In coincidence with this chronology is the occurrence of buried floodplain soils in the downstream Byelorussian section of the valley dated between 6.5 and 5.5 ka cal BP (^{14}C dates 5450 ± 170 and 5040 ± 110) (Kalicki and Sańko, 1992, 1998). The Mid-Holocene drop of fluvial activity at the Upper Dnieper was interrupted by period of high floods around the Subboreal-Subatlantic transition. Summary of high and low activity dates provided its constraints between 3.0 and 2.3 ka cal BP, though a number of dates that post-date high-flood events extend to less than 2.0 ka cal BP (**Fig. 5c**). Probably in favor of some younger limit of this high flood epoch is occurrence of buried floodplain soil between Orsha and Shklov dated between 2.3–2.0 ka cal BP (^{14}C date 940 ± 90) (Kalicki and Sańko, 1992, 1998).

Dnieper palaeohydrology in the Middle and Late Holocene corresponds well to changes of water regime in the sources of Volga and Western Dvina rivers catchments, which was estimated from the location of stationary ancient settlements in river valleys (Panin and Nefedov, 2010). In the Neolithic and Bronze Age (8–5 and 5–2.8 ka cal BP, respectively) a big part of settlements was located at the present-day floodplain elevations above rivers, *i.e.* within the action of modern floods. It proves that during these epochs intervals with low floods were prevailing. For the Late Holocene, contrasting hydrological changes were characteristic. In the Early Iron Age (2.8–1.8 ka cal BP), settlements occupied the highest position throughout the Holocene, and the percentage of settlements on low altitudes was minimal, which can be associated with the extremely high flood levels in that time. In the Middle Ages (1.8–0.3 ka cal BP), the percentage of settlements on modern floodplains rose considerably, which indicates the occurrence of long enough time intervals characterized by low floods. In general, this succession of palaeoflood changes is quite similar to that established in this paper in the Upper Dnieper from absolute dating.

Prominent feature of the Late Holocene palaeohydrology is the occurrence of the nearly millennium-long period (since between 2.3 (2.0) ka cal BP) when river floodplains had not been inundated. The Early Medieval low-flood period was reported from all over the central East European Plain (Butakov *et al.*, 2000) with the Upper Dnieper River being the westernmost location. Floodplain inundation at the upper Dnieper resumed around the XII-XIII century boundary (date no.7 in **Table 2**). Presumably similar chronology has been found in the Dnieper floodplain at Orsha (Byelorussia) where organic and peaty silts on floodplain were buried by overbank silty sands after 940 ± 90 BP (uncal) which has been regarded as the effect of deforestation (Kalicki and Sańko, 1992, 1998; Kalicki *et al.*, 2008). Nevertheless, rough contemporaneity of the rise in flood activity over the centre of the East European Plain evidences rather climatic than anthropogenic factors to be responsible for that. In the south-western regions of the East European Plain chronology of flood activity is some different: in the X–XII century AD a high frequency of floods is reported from the Upper Dniester River basin within the Eastern Carpathian foreland, Western Ukraine (Gębica *et al.*, 2013). On the contrary, low floods at the Upper Dnieper around the 10th century AD promoted establishing stationary settlements on its floodplain such as the above-mentioned

Gnezdovo settlement at the portage routes through the Dvina-Dnieper divide.

Gnezdovo flourished in the Dnieper valley in the 9–10th centuries AD. After more than a century lasting archaeological excavations, it was only in 1995 that a large portion of the settlement was unraveled within the Dnieper floodplain (Pushkina *et al.*, 2001). The artifact-bearing horizon(s) is buried under 1–3 m of overbank alluvium — the result of flood rise after the settlement decline in the mid-11th century. A covering of the cultural layer with overbank fines had hidden it from archaeologists but, on the other hand, it preserved the artifacts and alluvial stratigraphy in pristine conditions providing opportunities for detailed reconstructions.

ACKNOWLEDGEMENTS

The authors express their gratitude to the leaders of the Gnezdovo archaeological expedition Tamara Pushkina (Faculty of History, Lomonosov Moscow State University) and Veronica Murasheva (State Historical Museum, Moscow) for the initiative to establish geomorphic and absolute dating research program at the Gnezdovo archaeological site, and their long-lived support of this program. Starting at Gnezdovo, the author's interests spread over the whole Upper Dnieper region. Financial support for the studies summarized in the paper was received from the Russian Foundation for Basic Research (RFBR), projects no. 06-05-65218, 09-05-00340. The final part of the study (OSL dating and data synthesis) contributes to the current RFBR project no. 12-05-01148.

REFERENCES

Aleksandroskiy AL, Krenke NA and Nefedov VS, 2005. Paleorelief vysokoy poimy Dnepra na territorii Gnezdovskogo archeologicheskogo kompleksa (Paleotopography of the Dnieper River high floodplain at the Gnezdovo archaeological site). *Rossiyskaya Archeologia* 1: 112–123 (in Russian).

Arbogast AF, Bookout JR, Schrotenboer BR, Lansdale A, Rust GL and Bato VA, 2008. Post-glacial fluvial response and landform development in the upper Muskegon River valley in North-Central Lower Michigan, U.S.A. *Geomorphology* 102(3–4): 615–623, DOI 10.1016/j.geomorph.2008.06.008.

Barashkova ZK, Lavrovich ON, Briukov IP and Shuleshkina EA, 1998. *Karta chetvertichnykh otlozheniy Smolenskoy oblasti (Map of Quaternary deposits, the Smolensk Region, scale 1:500000)*. Ministry of Natural Resources of Russia (in Russian).

Belyaev VR, Golosov VN, Markelov, MV, Evrard O, Ivanova NN, Paramonova TA and Shamshurina EN, 2013. Using Chernobyl-derived ^{137}Cs to document recent sediment deposition rates on the River Plava floodplain (Central European Russia). *Hydrological Processes* 27(6): 807–821, DOI 10.1002/hyp.9461.

Borisova O, Sidorchuk A and Panin A, 2006. Palaeohydrology of the Seim River basin, Mid-Russian Upland, based on palaeochannel morphology and palynological data. *Catena* 66(1–2): 53–73, DOI 10.1016/j.catena.2005.07.010.

Bronk Ramsey C, 2009. Bayesian analysis of radiocarbon dates. *Radiocarbon* 51(1): 337–360.

Bronnikova MA and Uspenskaya ON, 2007. *Pozdnegolocenovaya evolutcia rastitel'nosti i landshafta na teritorii Gnezdovskogo archeologicheskogo kompleksa (Vegetation and landscape changes at the Gnezdovo archaeological site in the Late Holocene).* Gnezdovo: resul'taty kompleksnykh issledovaniy pamiatnika. Murasheva VV, ed. Moscow, State Historical Museum: 162–182 (in Russian).

Bronnikova MA, Zazovskaya EP and Bobrov AA, 2003. Local landscape evolution related to human impact of an early medieval pre-urban center in the Upper Dnieper region (Central Russian Plain): an interdisciplinary experience. *Revista Mexicana de Ciencias Geológicas* 20(3): 245–262.

Butakov GP, Kutbanova SG, Panin AV, Perevoschikov AA and Serebrennikova IA, 2000. Formirovanie antropogenno obuslovlennogo nailka na poimakh rek Russkoi ravniny (Human-induced alluviation on river floodplains in the Russian Plain). In: Erosionnye i Ruslovye Processy, Issue 3, Moscow, MSU Press: 78–92.

Gębica P, 2011. Stratigraphy of alluvial fills and phases of the Holocene floods in the lower Wislok river, SE Poland. *Geographia Polonica* 84, Special Issue Part I: 39–60.

Gębica P, 2013. Chronostratigraphy of alluvia and age of fluvial landforms in the Carpathian Foreland during the Vistulian. *Studia Quaternaria* 30(1): 19–27.

Gębica P, Szczepanek K and Wieczorek D, 2009. Late Vistulian alluvial filling in the San River valley in the Carpathian foreland (north of Jarosław town). *Studia Geomorphologica Carpatho-Balcanica* XLIII: 39–61.

Gębica P, Starkel L, Jacysyn A and Krapiec M, 2013. Medieval accumulation in the Upper Dniester river valley: the role of human impact and climate change in the Carpathian foreland. *Quaternary International* 293: 207–218, DOI 10.1016/j.quaint.2012.05.046.

Golosov VN, 2009. Issledovania akkumulacii nanosov na poimakh rek: potencial'nie metody I perspektivy (Investigations of sediment deposition on the floodplains: Potentials of methods and perspectives). *Geomorfologiya* 4: 39–45 (in Russian).

Harden T, Macklin MG and Baker VR, 2010. Holocene flood histories in south-western USA. *Earth Surface Processes and Landforms* 35(6): 707–716, DOI 10.1002/esp.1983.

Hoffmann T, Lang A and Dikau R, 2008. Holocene river activity: analysing 14C-dated fluvial and colluvial sediments from Germany. *Quaternary Science Reviews* 27(21–22): 2031–2040, DOI 10.1016/j.quascirev.2008.06.014.

Howard AJ, Macklin MG, Bailey DW, Mills S and Andreescu R, 2004. Late-glacial and Holocene river development in the Teleorman Valley on the southern Romanian Plain. *Journal of Quaternary Science* 19(3): 271–280, DOI 10.1002/jqs.805.

Johnstone E, Macklin M and Lewin J, 2006. The development and application of a database of radiocarbon-dated Holocene fluvial deposits in Great Britain. *Catena* 66(1–2): 14–23, DOI 10.1016/j.catena.2005.07.006.

Kalicki T, 1995. Late Glacial and Holocene evolution of some river valleys in Byelorussia. *Paläoklimaforschung* 14: 89–100.

Kalicki T, 2006. Zapis zmian klimatu oraz działalności człowieka i ich rola w holoceńskiej ewolucji dolin środkowoeuropejskich (Reflection of climatic changes and human activity and their role in the Holocene evolution of Central European valleys). *Prace Geograficzne Nr 204 (Geographical Studies No.204).* IGiPZ PAN, Warszawa, 2006. 348 p.

Kalicki T and Sańko A, 1992. Genesis and age of terraces of the Dnieper River between Orsha and Shklow, Byelorussia. *Geographia Polonica* 60: 151–174.

Kalicki T and Sańko AF, 1998. Palaeohydrological changes in the upper Dneper valley during the last 20 000 years (Belarus). In: *Palaeohydrology and Environmental Change* (G. Benito, V. R. Baker, K. J. Gregory, eds), Wiley, Chichester: 125–135.

Kalicki T, Sauchyk S, Calderoni G and Simakova G, 2008. Climatic versus human impact on the Holocene sedimentation in river valleys of different order: Examples from the upper Dnieper basin, Belarus. *Quaternary International* 189(1): 91–105, DOI 10.1016/j.quaint.2007.09.028.

Kasse C, Bohncke SJP, Vandenberghe J and Gábris G, 2010. Fluvial style changes during the last glacial–interglacial transition in the middle Tisza valley (Hungary). *Proceedings of the Geologists' Association* 121(2): 180–194.

Kvasov DD, 1979. The Late Quaternary history of large lakes and inland seas of Eastern Europe. *Annales Academiae Fennicae. Ser. A III* 12: 1–71.

Lang A, 2003. Phases of soil erosion-derived colluviation in the loess hills of South Germany. *Catena* 51(3–4): 209–221, DOI 10.1016/S0341-8162(02)00166-2.

Leigh DS, 2006. Terminal Pleistocene braided to meandering transition in rivers of the Southeastern USA. *Catena* 66(1–2): 155–160, DOI 10.1016/j.catena.2005.11.008.

Lericolais G, Guichard F, Morigi C, Popescu I, Bulois C, Gillet H and Ryan WBF, 2011. Assessment of Black Sea water-level fluctuations since the Last Glacial Maximum. *Geological Society of America Special Papers* 473: 33–50.

Lericolais G, Guichard F, Morigi C, Minereau A, Popescu I and Radan S, 2010. A post Younger Dryas Black Sea regression identified from sequence stratigraphy correlated to core analysis and dating. *Quaternary International* 225(1): 199–209, DOI 10.1016/j.quaint.2010.02.003.

Lewin J, Macklin MG and Johnstone EC, 2005. Interpreting alluvial archives: sedimentological factors in the British Holocene fluvial record. *Quaternary Science Reviews* 24(16–17): 1873–1889, DOI 10.1016/j.quascirev.2005.01.009.

Macklin MG, Benito G, Gregory KJ, Johnstone E, Lewin J, Michczynska DJ, Soja R, Starkel L and Thorndycraft VR, 2006. Past hydrological events reflected in the Holocene fluvial record of Europe. *Catena* 66(1–2): 145–154, DOI 10.1016/j.catena.2005.07.015.

Macklin MG and Lewin J, 1993. Holocene river alluviation in Britain. *Zeitschrift für Geomorphologie, Supplementbände* 88: 109–122.

Macklin MG, Johnstone E and Lewin J, 2005. Pervasive and long-term forcing of Holocene river instability and flooding in Great Britain by centennial-scale climate change. *The Holocene* 15(7): 937–943, DOI 10.1191/0959683605hl867ft.

Macklin MG and Lewin J, 2003. River sediments, great floods and centennial-scale Holocene climate change. *Journal of Quaternary Science* 18(2): 101–105, DOI 10.1002/jqs.751.

Major CO, Goldstein SL, Ryan WBF, Lericolais G, Piotrowski AM and Hajdas I, 2006. The co-evolution of Black Sea level and composition through the last deglaciation and its paleoclimatic significance. *Quaternary Science Reviews* 25(17–18): 2031–2047, DOI 10.1016/j.quascirev.2006.01.032.

Murasheva VV, Panin AV and Fetisov AA, 2009. *Mezhdisciplinarnye issledovania v arkheologii (po rezul'tatam issledovania Gnezdovskogo arkheologicheskogo kompleksa* (Multi-disciplinary investigations in archaeology: the Gnezdovo archaeological site case study. *Srednie Veka* 70(3): 132–147 (in Russian).

Panin AV, Fuzeina JN and Belyaev VR, 2009. Long-term development of Holocene and Pleistocene gullies in the Protva River basin, Central Russia. *Geomorphology* 108(1–2): 71–91, DOI 10.1016/j.geomorph.2008.06.017.

Panin AV, Sidorchuk AJ, Baslerov SV, Borisova OK, Kovaliukh NN and Sheremetskaya ED, 2001. Osnovnye etapy istorii rechnykh dolin centra Russkoy ravniny v pozdnem valdae I Holocene (Main stages of river valley development in the centre of the Russian Plain in the Late Valdai – Holocene time). *Geomorfologia* 2: 19–34 (in Russian).

Panin AV and Nefedov VS, 2010. Analysis of Variations in the Regime of Rivers and Lakes in the Upper Volga and Upper Zapadnaya Dvina Based on Archaeological–Geomorphological Data. *Water Resources* 37(1): 16–32.

Pushkina TA, Murasheva VV and Nefedov VS, 2001. Novoe v izuchenii central'nogo selischa v Gnezdove (New studies of the Central settlement in Gnezdovo). *Trudy GIM, 124.Gnezdovo: 125 let izychenia pamyatnika*. Moscow: 12–26 (in Russian).

Reimer PJ, Baillie MGL, Bard E, Bayliss A, Beck JW, Blackwell PG Bronk Ramsey C, Buck CE, Burr GS, Edwards R, Friedrich M, Grootes PM, Guilderson, TP Hajdas I Heaton TJ Hogg AG, Hughen KA, Kaiser KF, Kromer B, Manning FG, McCormac SW, Reimer RW, Richards DA, Southon JR, Talamo S, Turney CSM van der Plicht J and Weyhenmeyer CE, 2009. IntCal09 and Marine09 radiocarbon age calibration curves, 0–50,000 years cal BP. *Radiocarbon* 51(4): 1111–1150.

Salov IN, 1972. Granitsy Moscovskogo i Valdaiskogo lednikovykh schitov v ikh maksimal'nye phasy v Byelorussu i v Smolenskoy oblasti i ikh konechno-morennye compleksy (Boundaries of Moscovian and Valdaian ice sheets at their maximal phases in Byelirussia and Smolensk Region, and their end-morain complexes). In: *Kraevye obrazovania materikovykh oledeneniy*. Moscow: Nauka: 145–154 (in Russian).

Sidorchuk AY, Panin AV and Borisova OK, 2011. Surface runoff to the Black Sea from the East European Plain during Last Glacial Maximum — Lat Glacial time. *Geological Society of America Special Papers* 473: 1–25.

Sidorchuk A, Panin A and Borisova O, 2009. Morphology of river channels and surface runoff in the Volga River basin (East European Plain) during the Late Glacial period. *Geomorphology* 113(3–4): 137–157, DOI 10.1016/j.geomorph.2009.03.007.

Sidorchuk AY, Panin AV and Borisova OK, 2012. River Runoff Decrease in North Eurasian Plains during the Holocene Optimum. *Water Resources* 39(1): 69–81.

Starkel L and Gębica P, 1995. Evolution of river valleys in southern Poland during the Pleistocene-Holocene transition. *Biuletyn Peryglacjalny* 34: 177–190.

Starkel L, Kalicki T, Krąpiec M, Soja R, Gębica P and Czyżowska E, 1996. Hydrological changes of valley floor in the Upper Vistula basin during Late Vistulian and Holocene. In L. Starkel (Ed.), Evolution of the Vistula river valley during the last 15 000 years. *Quaestiones Geographicae*, Special Issue 9: 7–128.

Starkel L, Soja R, Michczynska DJ, 2006. Past hydrological events reflected in Holocene history of Polish rivers. *Catena* 66(1–2): 24–33, DOI 10.1016/j.catena.2005.07.008.

Stolyarova TI, 1970. *Karta chetvertichnykh otlozheniy, kvadrat N-36-VIII, masshtab 1 : 200 000* (Map of Quaternary deposits, quadrangle N-36-VIII, scale 1 : 200 000). Moscow; VAGT MinGeo USSR (in Russian).

Sukhodolov AN, Arnaut NA, Kudersky LA, Loboda NS, Bekh VV, Skakalsky BG, Katolikov VM and Usatii MA, 2009. Western Steppic Rivers. In: *Rivers of Europe* (K.Tockner, U.Uehlinger, C.T. Robinson, eds). Elsevier-Academic Press, Amsterdam: 497–523.

Szumanski A, 1983. Paleochannels of large meanders in the river valleys of the Polish lowland. *Quaternary Studies in Poland* 4: 207–216.

Szumanski A, 1986. Postglacjalna ewolucja i mechanism transformacji dna doliny dolnego sanu (Post Glacial evolution and mechanizm of transformation of a floor of the lower San valley). *Kwartalnik AGH, Geologia* 12(1): 1–92.

Thorndycraft VR and Benito G, 2006. The Holocene fluvial chronology of Spain: evidence from a newly compiled radiocarbon database. *Quaternary Science Reviews* 25(3–4): 223–234, DOI 10.1016/j.quascirev.2005.07.003.

Vandenberghe J, Kasse C, Bohncke SJP and Kozarski S, 1994. Climate-related river activity at the Weichselian–Holocene transition: a comparative study of the Warta and Maas rivers. *Terra Nova* 6: 476–485.